Molecular Therapy
Methods & Clinical Development
Original Article

AAV2/8 Anti-angiogenic Gene Therapy Using Single-Chain Antibodies Inhibits Murine Choroidal Neovascularization

Chris P. Hughes,[1] Neil M.J. O'Flynn,[1] Maureen Gatherer,[1] Michelle E. McClements,[2] Jennifer A. Scott,[1] Robert E. MacLaren,[2] Srinivas Goverdhan,[1] Martin J. Glennie,[3] and Andrew J. Lotery[1]

[1]Clinical Neurosciences, Faculty of Medicine, University of Southampton, Southampton, UK; [2]Oxford Eye Hospital and Nuffield Laboratory of Ophthalmology, Nuffield Department of Clinical Neurosciences, University of Oxford, Oxford, UK; [3]Cancer Sciences, Faculty of Medicine, University of Southampton, Southampton, UK

While anti-angiogenic therapies for wet age-related macular degeneration (AMD) are effective for many patients, they require multiple injections and are expensive and prone to complications. Gene therapy could be an elegant solution for this problem by providing a long-term source of anti-angiogenic proteins after a single administration. Another potential issue with current therapeutic proteins containing a fragment crystallizable (Fc) domain (such as whole antibodies like bevacizumab) is the induction of an unwanted immune response. In wet AMD, a low level of inflammation is already present, so to avoid exacerbation of disease by the therapeutic protein, we propose single-chain fragment variable (scFv) antibodies, which lack the Fc domain, as a safer alternative. To investigate the feasibility of this, anti-vascular endothelial growth factor (VEGF)-blocking antibodies in two formats were produced and tested *in vitro* and *in vivo*. The scFv transgene was then cloned into an adeno-associated virus (AAV) vector. A therapeutic effect in a mouse model of choroidal neovascularization (CNV) was demonstrated with antibodies in both scFv and immunoglobulin G1 (IgG1) formats ($p < 0.04$). Importantly, the scFv anti-VEGF antibody expressed from an AAV vector also had a significant beneficial effect ($p = 0.02$), providing valuable preclinical data for future translation to the clinic.

INTRODUCTION

Age-related macular degeneration (AMD) affects nearly 50 million individuals globally,[1] costing $2 billion per year. With an aging population, this is predicted to increase to $20 billion over the next decade, thus putting increasing, possibly unsustainable, financial demand on health care systems.[2] Disease is characterized by excessive angiogenesis, causing irreversible loss of central vision.[1] Therefore, treatments have targeted the inhibition of this pathway. Current therapeutics for wet AMD have short half-lives, which necessitates monthly or bimonthly injections into the eye in perpetuity. This is expensive, painful, and prone to adverse effects. Repeated injections can result in retinal detachment, endophthalmitis, cataract, and possibly irreversible geographic atrophy (GA) in the long term.[3] Gene therapy can revolutionize AMD treatment by drastically reducing administration frequencies. Several phase I clinical trials of gene therapy for wet AMD have been reported, including adeno-associated virus AAV2 carrying sFLT01 (soluble vascular endothelial growth factor [VEGF] receptor) by Rakoczy et al.[4,5] (ClinicalTrials.gov: NCT01678872).

In this study, we have utilized AAV, which has been shown to be safe in a number of clinical trials to date, and, compared to lentiviruses, it has a significantly lower insertional mutagenesis risk.[6] The absence of a cell-derived envelope makes AAV less immunogenic than many other viral vectors (such as adenovirus), and it has also demonstrated long-term expression in retinal cells.[7] Indeed, many forms of therapeutics have been delivered by AAV for use in AMD models, ranging from anti-VEGF antibodies,[8] anti-VEGF small hairpin RNA (shRNA),[9] and sFlt-1[10] to soluble membrane attack complex inhibitory protein (sCD59).[11] AAV has also been tested in several landmark ocular gene therapy clinical trials, including a phase I/II clinical trial for choroideremia where the vector was successfully delivered to the macula.[12] To date, all trials published with AAV-mediated gene therapy for eye diseases have used the AAV2 serotype. However, quicker and higher transgene expression levels may occur with AAV2/8 vectors after subretinal injection.[13] We reasoned that the greatest expression of anti-angiogenic agents would equate to best efficacy; therefore, we chose the AAV8 serotype for this study. After subretinal injection, AAV2/8 transduces mainly retinal pigmented epithelium (RPE) cells and some photoreceptors.[13]

We have recently shown that Fcγ receptor upregulation produces immune complex-mediated inflammation in AMD.[14] This may have implications for therapy with agents that have Fc segments. Therapeutic agents such as single-chain fragment variable (scFv) antibodies that do not exacerbate disease by activating Fc receptors and complement would be preferable. scFv antibodies consist of only V_H and V_L

Received 13 June 2018; accepted 16 November 2018;
https://doi.org/10.1016/j.omtm.2018.11.005.

Correspondence: Andrew J. Lotery, Clinical Neurosciences, Faculty of Medicine, University of Southampton, South Lab and Path Block, MP 806, Level D, Southampton General Hospital, Tremona Road, Southampton SO16 6YD, UK.
E-mail: a.j.lotery@soton.ac.uk

 Crown Copyright © 2019
This is an open access article under the CC BY-NC-ND license (http://creativecommons.org/licenses/by-nc-nd/4.0/).

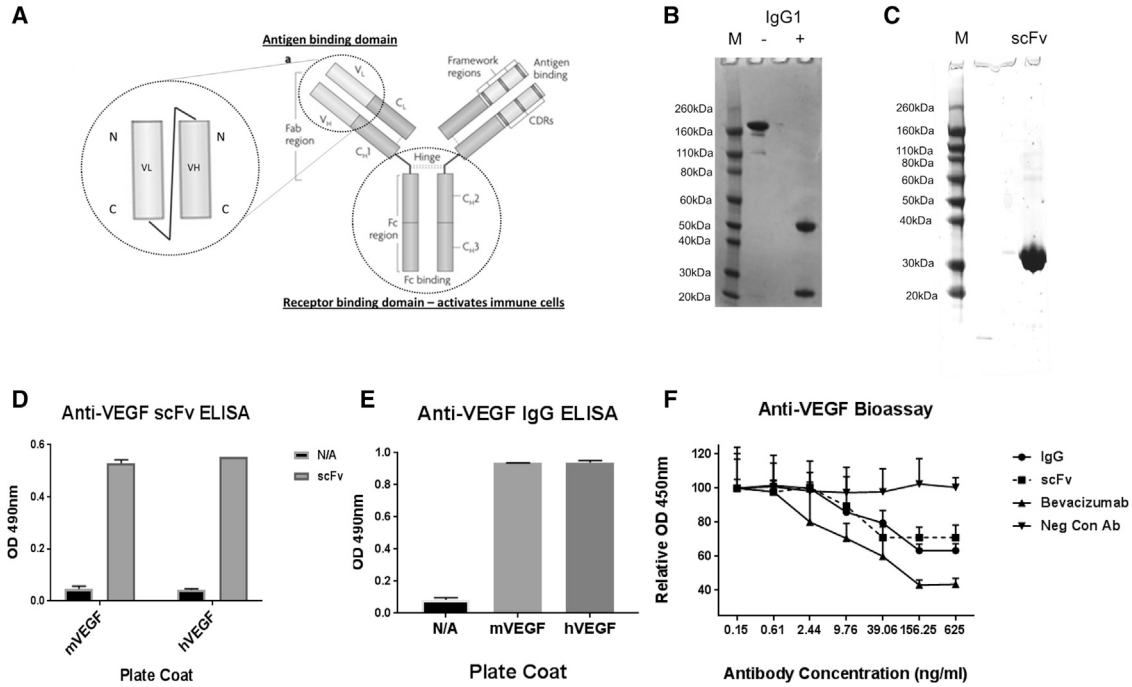

Figure 1. *In Vitro* Characterization of Recombinant Anti-VEGF Antibodies

(A) Schematic of the antibodies produced; to the left, a representation of the scFv format, and to the right, the full IgG format, adapted from Hansel et al.[35] (B) SDS-PAGE analysis of the anti-VEGF IgG1 format. The expected single 160-kDa band of the IgG1 antibody was observed in the absence of mercaptoethanol (–), while, in the presence of mercaptoethanol (+), dissociation into the heavy (55 kDa) and light chains (25 kDa) was seen. M refers to protein marker. (C) SDS-PAGE analysis of the anti-VEGF scFv format. The anti-VEGF scFv migrated at around 30 kDa (predicted molecular weight [MW] = 32 kDa). (D and E) Antigen specificity of anti-VEGF antibodies. Binding of anti-VEGF antibodies to human or murine VEGF-coated ELISA plates was detected by anti-His for scFv (D) or anti-mouse HRP for IgG1 (E). Both formats of anti-VEGF and specifically bound both mouse and hVEGF. N/A refers to a control where no sample was added to the plate. N/C refers to a control where no VEGF was added to the plate. Bars represent the mean of samples that were added in duplicate, and error bars represent the SD. (F) Biological activity of anti-VEGF antibodies (bioassay). VEGF-dependent growth of HDMECs was blocked by adding increasing amounts of anti-VEGF antibody to the cells. The IgG and scFv forms of anti-VEGF as well as the positive control anti-VEGF (bevacizumab) were able to block growth in a dose-dependent fashion, indicating activity. The negative control (Neg Con Ab, an anti-PDGFR-β IgG1) was not active. Data points represent the mean of samples that were added in triplicate, and error bars represent the SD. Values are presented as percent relative to the first data point (0.2 ng/mL antibody).

domains separated by a flexible linker (see Figure 1A), and they represent the minimum portion of an antibody required for antigen binding.[15] We believe the development of scFv antibodies is important, as they are smaller (cDNA ~1 kb) than whole antibodies (~2.5 kb) or Fab fragments, and so they are better suited to expression from AAV vectors with limited transgene capacity (<5 kb). Indeed, it is theoretically possible to fit more than one scFv into the same AAV vector, which opens up possibilities for combination therapies. Smaller scFv antibodies may also have improved diffusion *in vivo* compared to larger standard antibodies,[16] thus acting on a greater area of the retina. An anti-VEGF designed ankyrin repeat protein (DARPin) has been successfully used in AMD models,[17] and it is now being evaluated in clinical trials.[18] In addition, an alternative class of antibodies, the camelid-derived nanobodies are in several trials (e.g., anti-IL-6R for autoimmune diseases[19]). However, we are unaware of any reports of anti-angiogenic antibodies in the scFv format being developed for AMD. Therefore, this is both a novel and highly relevant option to developing a safer, longer lasting, and convenient therapy for AMD. Furthermore, the combination of anti-VEGF scFv with an AAV2/8 vector may translate to an improved gene therapy for wet AMD. The purpose of this study was to provide preclinical data for an AAV2/8 vector encoding a previously described G6-31 anti-VEGF antibody[20] in scFv format for possible translation as a novel therapy for AMD.

RESULTS

Production and *In Vitro* Testing of Recombinant Anti-VEGF Antibodies

The anti-VEGF antibodies used in this study were based on the G6-31 antibody described by Liang et al.[20] We incorporated the binding sites of G6-31 into both a standard (immunoglobulin G1 [IgG1]) and scFv format, and we evaluated these antibodies for effectiveness in treating a laser-induced choroidal neovascularization (CNV) mouse model. The IgG1 antibody protein was produced by transfecting 293F cells with a plasmid containing both the heavy and light chains that later associate to form the mature IgG1 (see Figure 1A for illustration of antibodies used in this study). The scFv (variable heavy and variable light chains only) was encoded in a

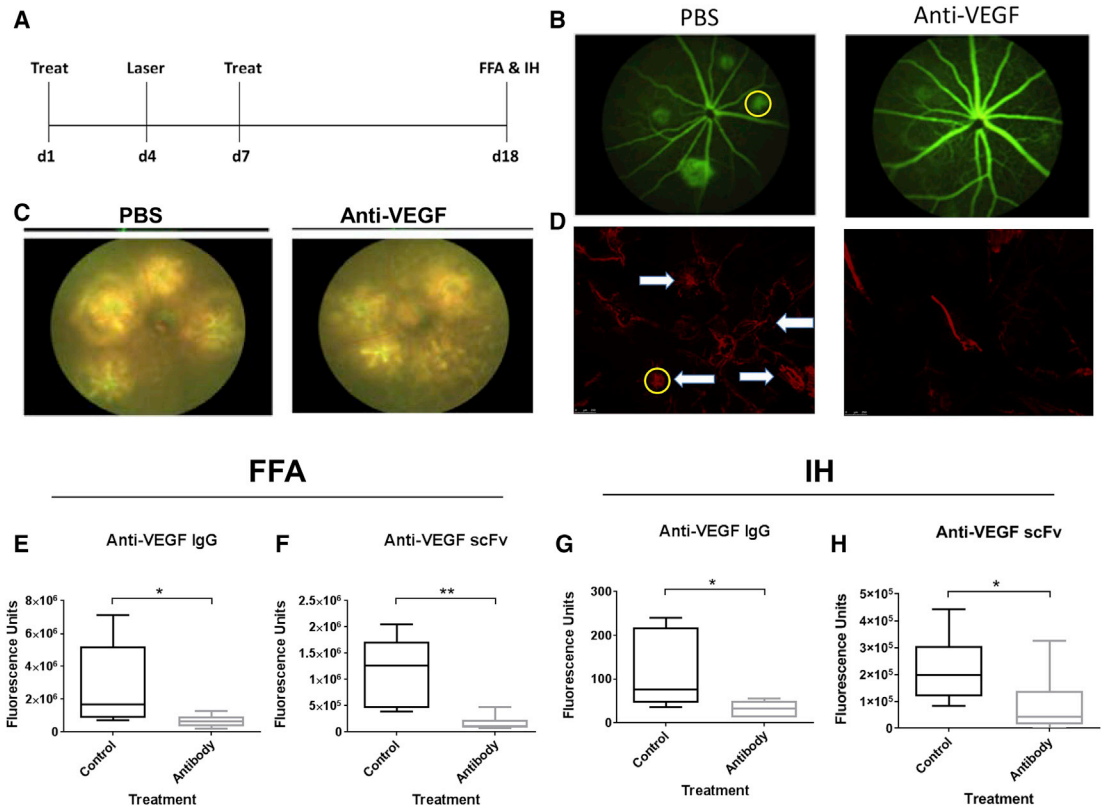

Figure 2. *In Vivo* Activity of Recombinant Anti-VEGF Antibodies

(A) Representation of timeline of antibody treatment experiments. Treat, antibody injection; laser, CNV induction; d, days. Times of FFA and culling mice for IH are indicated. (B–D) Representative images of the CNV treatment experiment. 14 days after laser administration, a decrease in neovascularization was seen with antibody injection compared to PBS, both as determined by FFA (B) and by collagen IV staining by IH (D); white arrows indicate lesions. Yellow circles on PBS-treated images illustrate a typical region of interest used to quantify fluorescence signal. (C) Fundus photograph images showing laser marks. (E and G) *In vivo* activity of IgG1 anti-VEGF. Mice were treated with 40 μg antibody, both 3 days before and 3 days after laser induction of CNV. 14 days after laser administration, CNV lesions were measured by FFA (E) and IH (G). Signals were quantified using ImageJ. A significantly lower fluorescence signal was observed with IgG1 anti-VEGF treatment than with PBS using both methods (using Mann-Whitney test, n = 5 eyes). (F and H) *In vivo* activity of scFv anti-VEGF. Mice were treated with the same dose of scFv antibody, and CNV lesions were quantified after FFA (F) or IH (H). A significantly lower fluorescence signal was observed with scFv anti-VEGF treatment than with PBS using both methods (using Mann-Whitney test, n = 6 eyes). *$p < 0.05$, **$p < 0.005$.

single plasmid and produced in a similar way. Both proteins gave high yields (>10 mg/L medium).

After purification, SDS-PAGE analysis demonstrated the expected molecular weight (160 kDa for IgG1 and 32 kDa for scFv) and high purity of both of the antibody formats (Figures 1B and 1C). Importantly, both antibodies were able to bind both human and mouse VEGF in ELISA (Figures 1D and 1E). The blocking activity of both antibody formats was also confirmed in a bioassay (Figure 1F). This assay used varying amounts of antibody to block the human VEGF-dependent growth of human dermal microvascular endothelial cells (HDMECs). A dose-dependent inhibition of cell growth in all anti-VEGF-treated cells was seen, but not with an irrelevant control antibody. Surprisingly, our IgG antibody had an inferior activity compared to our positive control antibody (bevacizumab), despite the affinity of bevacizumab being lower. This may be explained by the bevacizumab being taken from a clinical treatment vial, which may well be more pure and active than our preparations. Half-maximal inhibition of 10 ng/mL human VEGF occurred with approximately 10 ng/mL IgG and 40 ng/mL scFv anti-VEGF, while around 2 ng/mL was required for bevacizumab. Thus, the IgG is more active than the scFv, which reflects the higher affinity of the whole antibody format.

In Vivo Testing of Recombinant Anti-VEGF Antibodies

Antibody preparations were tested for endotoxin before injecting into mice. All samples were endotoxin negative (<10 endotoxin units [EUs]/mL/mg, data not shown). 40 μg anti-VEGF IgG1 protein was injected intravitreally both 3 days before and 3 days after laser induction of CNV (n = 5 eyes). At 2 weeks after laser injury, the therapeutic effect on CNV was investigated by fundus fluorescein angiography (FFA) and immunohistology (IH, staining eye cups for blood vessels). This experimental timeline is shown in Figure 2A.

Figures 2B and 2D show typical images from this experiment. In general, an excellent correlation was seen between FFA and IH, with lesions showing similar locations and intensity. In addition, four CNV spots were always observed in the untreated eyes, indicating the reliability of laser-induced lesions. Indeed, fundus photographs showed four marks in all lasered eyes, and so were used to confirm the presence of injury even in treated eyes without detectable lesions (Figure 2C). Moreover, on quantification of these signals (as illustrated with circles in Figures 2B and 2D) using ImageJ,[21] a significant ($p = 0.03$) decrease in CNV fluorescence (77%) was seen using FFA methods in IgG antibody-treated eyes (mean fluorescence units [FUs] = 640,000 ± SD 400,000), compared to PBS-injected controls (2,700,000 FUs ± 2,600,000; Figure 2E). An equally significant ($p = 0.03$) decrease (73%) was observed in antibody-injected eyes (32 FUs ± 18) compared to control eyes (120 FUs ± 90), as determined by IH (Figure 2G)

The anti-VEGF scFv was tested in the same way, using the same dose ($n = 6$ eyes). A significant ($p = 0.004$) decrease in fluorescein signal (85%) was detected in antibody-treated eyes (160,000 FUs ± 150,000; Figure 2F) versus PBS-treated eyes (1,200,000 FUs ± 660,000). Similarly, a significant ($p = 0.04$) reduction in collagen IV staining (61%), was noted in anti-VEGF scFv-administered eyes (84,000 FUs ± 120,000) relative to PBS controls (220,000 FUs ± 130,000; Figure 2H). Thus, the two antibody formats showed similar efficacies. The quantification data for individual animals treated with recombinant antibody are in Table S1.

Production and *In Vitro* Testing of AAV2/8 Anti-VEGF scFv Antibodies

The AAV2/8 vector (illustrated in Figure 3A) was designed for maximal transgene expression, with a strong CAG (cytomegalovirus early enhancer element, chicken beta-actin promoter, rabbit beta-globin gene) promoter[22] and a WPRE (woodchuck hepatitis virus post-transcriptional regulatory element) sequence[23] to enhance expression. As well as the anti-VEGF scFv, another scFv (termed Bcl-1, of unknown specificity) was cloned into a separate vector as a negative control. Purified AAV2/8 scFv was verified by confirming the presence of the three main AAV proteins (VP1, VP2, and VP3) using SDS-PAGE (data not shown). The virus was titered by qPCR, and HEK293T cells were infected (at an MOI of 100,000:1) to test the expression of antibody. The supernatant of infected HEK293T cells was analyzed, and the expressions of both antibodies by western blot were detected (data not shown). Importantly, this supernatant was found to contain VEGF-binding activity by ELISA (Figure 3B), indicating that the anti-VEGF scFv had been correctly expressed and secreted and was functional. Moreover, the negative control antibody did not bind VEGF in this ELISA (Figure 3B).

In Vivo Testing of AAV2/8 Anti-VEGF scFv Antibodies

To test expression from the AAV2/8 vectors *in vivo*, each mouse was injected with 8×10^8 genome copies (gcs) of AAV2/8 anti-VEGF scFv in one eye and equal amounts of AAV2/8 control scFv in the other eye. These were given subretinally to maximize expression, as expression of AAV2/8 vectors is around 10-fold higher than the intravitreal route.[13] At 4 months after injection, eyes were analyzed for antibody expression by western blot ($n = 3$) and ELISA ($n = 2$). Anti-VEGF scFv could be detected in ELISA (Figure 3C). The quantity of antibody was then estimated at approximately 1,000 μg/mL by extrapolating the signal obtained relative to that from a known concentration of anti-VEGF scFv protein (Figure 3C). Some anti-VEGF was also detected in one of the control AAV-treated eyes, although at much lower levels. Similarly, anti-VEGF was detected in the serum of one of the two mice at very low levels (20-fold less than the injected eye). Importantly, supernatant from AAV control scFv (Bcl)-infected cells did not bind VEGF in ELISA (Figure 3B). Western blot showed the expected molecular weight bands (32 kDa) in anti-VEGF scFv and control scFv eyes (Figure 3D). In contrast to the ELISA (which cannot detect the control scFv), western blot resulted in bands of similar intensities in AAV anti-VEGF and AAV control scFv. This was to be expected, as the western blot detects both anti-VEGF and control scFv (via their His tags), and equal amounts of each virus were injected into both eyes.

Once the presence of anti-VEGF had been shown in the AAV-injected eyes, the exact localization of transduced cells was next investigated using immunohistochemistry (IHC). Sections of AAV anti-VEGF- and PBS-injected control eyes (posterior poles only) were stained with DAPI (blue) so that the various tissues could be visualized. Typical confocal images (Figure 3E) showed green staining when slides were incubated with an anti-His tag (which is incorporated into the anti-VEGF) antibody and a fluorescently labeled secondary antibody. Importantly, there was no green signal in AAV anti-VEGF control sections with the secondary antibody alone or in PBS-injected eyes incubated with both detecting antibodies. This indicates a specific signal that corresponds to the anti-VEGF protein. Of note, the region of the eye stained was mainly the RPE. This in agreement with previous studies where subretinal injection of AAV2/8 vectors resulted in transduction largely of RPE cells, with some photoreceptors.[13]

When laser was used to induce CNV 3 weeks after AAV2/8 scFv injection (see Figure 4A for an illustration of AAV treatment timelines and Figure 4B for typical FFA images), a significant ($p = 0.02$) 83% decrease was seen in FFA CNV signal ($n = 7$ eyes) in AAV anti-VEGF eyes (480,000 FUs ± 1,000,000) compared to control AAV (2,800,000 FUs ± 2,600,000; Figure 4C). Moreover, when re-challenged with a repeat CNV laser induction in the same mice after a further 2 months, the anti-angiogenic effect (81% decrease in FFA signals) was as significant (720,000 FUs ± 750,000 for AAV anti-VEGF scFv versus 3,800,000 FUs ± 2,800,000 for control AAV; Figure 4D). A significant ($p = 0.03$, $n = 5$ eyes) decrease (67%) in CNV was also noted in AAV anti-VEGF eyes as determined by IH (2,400,000 FUs ± 1,300,000 for AAV anti-VEGF scFv versus 7,200,000 FUs ± 4,400,000 for control AAV) at the 2-month time point (Figure 4E). The quantification data for individual animals treated with AAV scFv are in Table S2. Together, these data indicate a long-term effect in these mice.

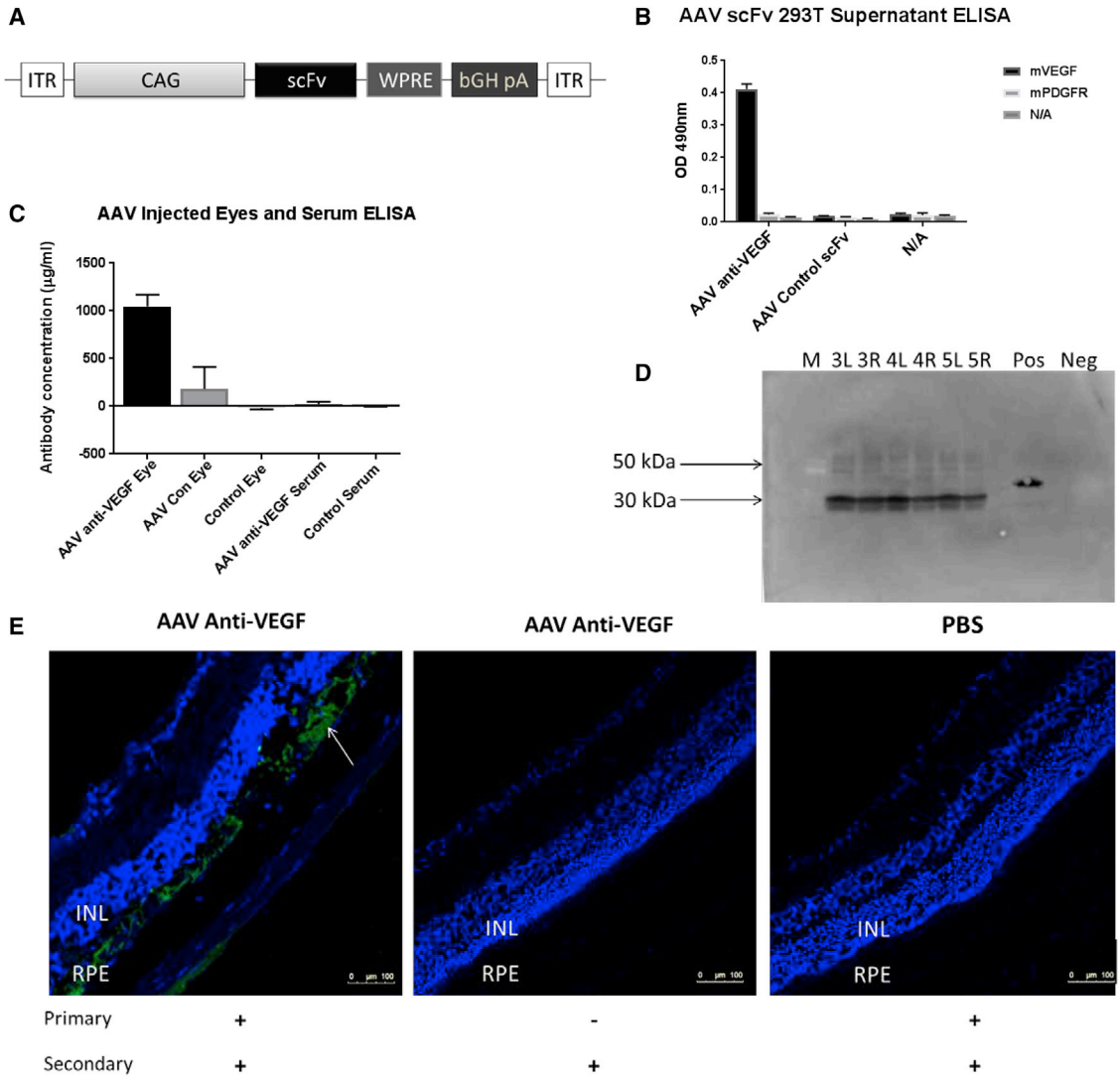

Figure 3. Characterization of AAV Anti-VEGF

(A) Schematic representation of AAV scFv vector. ITR, inverted terminal repeat of AAV2; CAG, synthetic ubiquitous promoter comprising the cytomegalovirus (CMV) early enhancer element, chicken beta-actin promoter including intron 1 fragments followed by intron 2-exon 3 fragments of the rabbit beta-globin gene (with splice features); scFv, single-chain antibody; WPRE, woodchuck post-transcriptional response element; bGH pA, bovine growth hormone polyadenylation signal. (B) Antigen specificity of anti-VEGF antibodies secreted by AAV scFv-infected cells. 293T cells were infected by AAVs carrying scFv antibodies to VEGF or an irrelevant control antibody, and the supernatants were assayed for activity by ELISA (as in Figure 1D). The plates were coated with either mVEGF or mouse platelet derived growth factor receptor (mPDGFR) as a negative control. N/A refers to a no-sample negative control. Anti-VEGF specifically bound to VEGF, while no signal was detected with the control antibody. Bars represent the mean of samples that were added in duplicate, and error bars represent the SD. (C) Expression of antibodies from AAV *in vivo*. Two mice were injected into their left eyes with AAV anti-VEGF scFv (AAV anti-VEGF Eye) and right eyes with AAV control antibody (AAV Con Eye). 4 months later, eyes and serum were harvested from injected mice. Serum (AAV anti-VEGF Serum) and homogenized eye samples were then analyzed for antibody expression by ELISA (as in Figure 1D). The concentration of anti-VEGF antibody of each sample was then determined by the signal given relative to that by a known concentration of anti-VEGF scFv protein. As negative controls, eyes (Control Eye) and serum (Control Serum) from an uninjected animal were used. (D) Demonstrating the presence of anti-VEGF in mouse eyes by western blot. Mice 3–5 (n = 3) were injected with AAV anti-VEGF (left eyes, L) or with AAV control antibody (Bcl, right eyes, R). Anti-His tag antibody used to detect anti-VEGF antibody. Pos, recombinant protein anti-VEGF scFv; neg, uninjected eye. Bands at the expected size confirm antibody expression in all homogenized eyes except the uninjected. Slightly larger size of bands in Pos compared to eyes can be explained by differences in glycosylation of the antibody. (E) Localization of antibodies from AAV *in vivo*. Expression of anti-VEGF was also confirmed by IHC. Sections of AAV anti-VEGF- and PBS control-injected eyes were stained with DAPI (blue) to visualize cell nuclei. Anti-VEGF was detected via its His tag, using a mouse anti-His primary antibody, followed by an anti-mouse Alexafluor 555 secondary antibody. Representative images taken with a confocal microscope are shown. Labels above indicate the material injected into the eye, and the detection antibodies used are shown below. Green staining (white arrow) corresponds to anti-VEGF, and it is mostly localized at the retinal pigmented epithelium (RPE). Also labeled for reference adjacent to the RPE is the inner nuclear layer (INL).

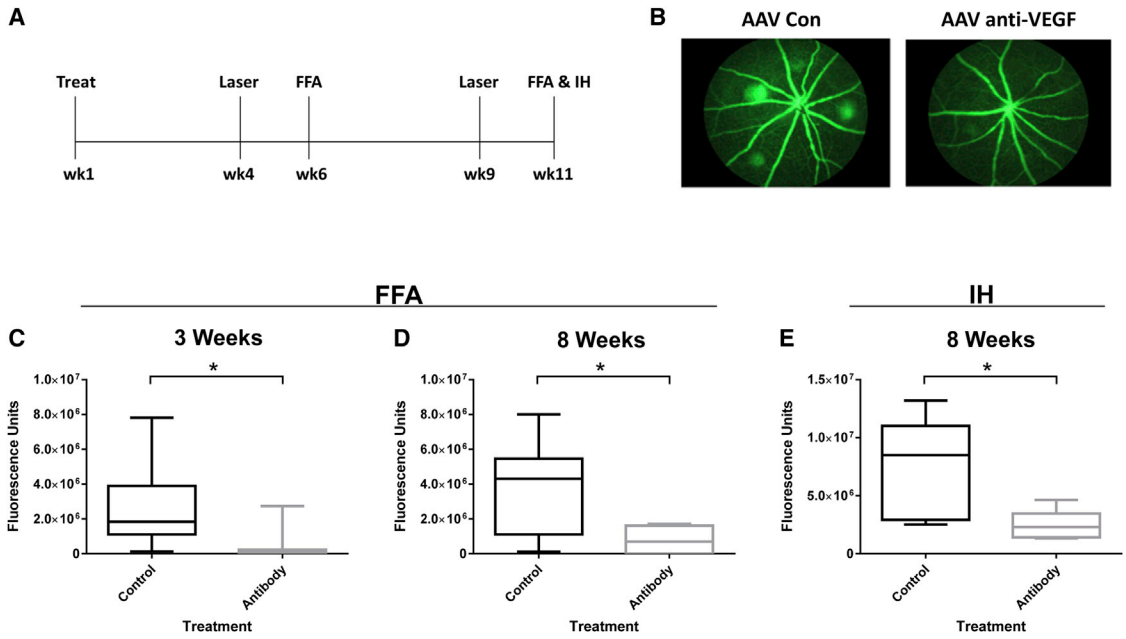

Figure 4. *In Vivo* Activity of AAV Anti-VEGF

(A) Representation of timeline of AAV treatment experiments. Treat, AAV injection; laser, CNV induction; wk, weeks; times of FFA or culling mice for IH are indicated. (B) Representative images of the CNV treatment experiment. An FFA picture is shown. (C and D) *In vivo* activity of AAV anti-VEGF scFv (by FFA). Effects on CNV were measured by FFA. Laser was applied at 3 weeks (C) and 8 weeks (D) post-AAV subretinal injection (in the same eyes). FFA was performed 2 weeks after laser administration. A significantly lower ($p = 0.02$) CNV fluorescence signal was observed with AAV anti-VEGF than with AAV control scFv ($n = 7$ eyes) at both time points. (E) *In vivo* activity of AAV anti-VEGF scFv (by IH). Effects on CNV were measured by IH. Laser was applied at 8 weeks post-injection, and IH was performed 2 weeks later. A significantly lower ($p = 0.03$) fluorescence signal was observed with anti-VEGF than with AAV control scFv ($n = 5$ eyes). Thus, long-lasting efficacy is seen using both FFA and IH. *p values < 0.05.

To demonstrate a lack of toxicity of injected AAV anti-VEGF, electroretinography (ERG) responses were obtained ($n = 4$ anti-VEGF study eyes, $n = 3$ PBS control eyes). No significant reduction in B wave amplitudes was revealed in the study and control eyes (0.11 versus 0.10 mV, $p = 0.34$). The mean A wave amplitude was reduced in study eyes marginally (−0.03 versus −0.01 mV, $p = 0.06$). The implicit times were unaffected and similar for both A waves and B waves in the study and control eyes (Figure 5A). To assess toxicity of the PF68 used as a surfactant in the previous AAV anti-VEGF efficacy experiment, PBS with or without PF68 was injected into eyes. PBS+ (with PF68; $n = 3$ eyes) and PBS (without PF68; $n = 3$ eyes) showed no significant differences in the B or A wave amplitudes and implicit times (Figure 5B).

DISCUSSION

This study describes the use of a novel anti-VEGF antibody format designed to develop gene therapy of wet AMD. This antibody was based on the G6-31 generated by Liang et al.,[20] and it was chosen as it was shown to bind both human and mouse forms of VEGF with high affinity. This binding was greater than that of bevacizumab[20] (K_d to human VEGF (hVEGF) of 0.2 nM for G6-31 IgG and 2.2 nM for bevacizumab). These are highly desirable features of a potential therapeutic agent, which can be tested in mouse models and progress rapidly to clinical trials without modification.

Moreover, this antibody in an IgG format had previously been shown to suppress CNV in mice after being given intraperitoneally.[24] However, this administration route has disadvantages if these methods were translated to treating AMD patients. These include a potential induction of an immune response by the IgG antibody and side effects of systemic VEGF suppression. Therefore, delivery into the immune-privileged eye appears more appropriate. To minimize the chances of the antibody causing deleterious inflammation in the eye, this antibody was produced in the mouse IgG1 format (as this isotype is the least able to activate complement or bind activating Fc receptors on antigen binding).

To validate the efficacy of the anti-VEGF, we first used purified proteins of the mouse immunoglobulin G Subclass 1 (mIgG1) and scFv formats. These proteins were then shown to bind both human and mouse forms of VEGF in ELISA. While we have not tested the affinities of our antibodies, we expect the affinity of our IgG1 antibodies to be similar to the IgG reported by Liang et al.,[20] i.e., 0.2 nM for hVEGF and 0.3 nM for mouse VEGF (mVEGF). While scFv antibodies were not studied by Liang et al.,[20] we can assume they will be similar to the affinities of the Fab they used, i.e., 0.9 nM for hVEGF and 0.6 nM for mVEGF. The affinity is higher for IgG than Fab and scFv, because the two binding sites in IgG create an extra avidity effect compared to the one binding site in Fab and scFv.

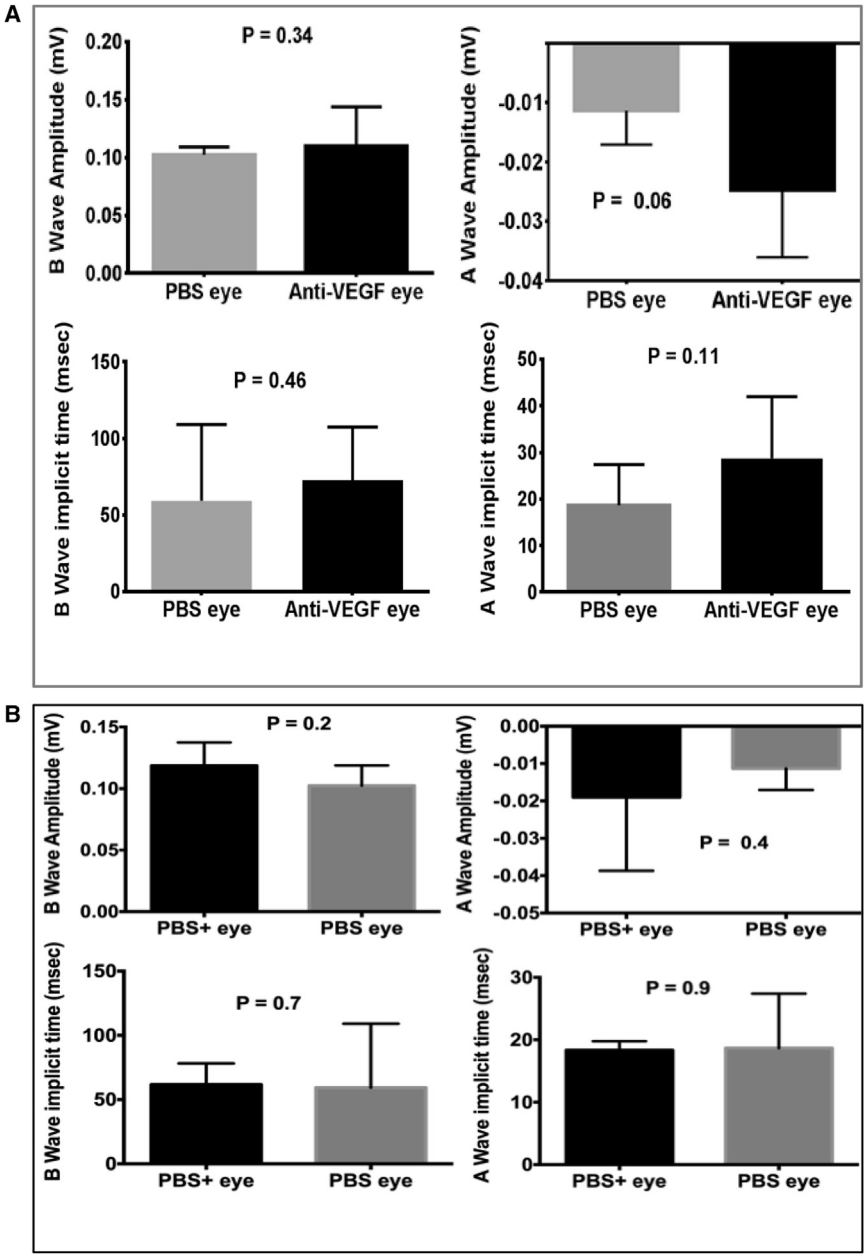

Figure 5. ERG Analysis of Injected Eyes

(A) ERG mean amplitudes and implicit times recorded in AAV anti-VEGF-injected study eyes (n = 4 mice) and PBS control eyes (n = 3 mice). (B) ERG mean amplitudes and implicit times recorded in PBS + PF68 surfactant- and PBS alone-injected eyes (n = 3 mice). p values shown (using Mann-Whitney 2-tailed test) are all >0.05, indicating that no statistically significant differences in signals were observed between any treatment and controls.

These antibodies were then shown to block VEGF activity *in vitro* and limit CNV *in vivo* after injection into the eye. Interestingly, a remarkably similar amount of inhibition of CNV was found with equal doses of the two different formats. This is very encouraging for potential clinical development of the scFv. It is tempting to directly compare the IgG and scFv versions in our experiments, but caution must be taken in interpretation of the data. A simple comparison of both *in vitro* and *in vivo* results even using equal amounts of protein of both antibodies is complicated by the different molecular weight of the antibodies; we estimate that approximately five times the number of scFv molecules (and 2.5 times the antibody-binding sites) are present per gram. Other factors to be taken into account are the advantage of possible enhanced diffusion to the outer retina of the smaller scFv format being balanced by disadvantages such as decreased affinity and a potentially shorter half-life of scFv compared to IgG antibodies.

The anti-VEGF scFv was incorporated into an AAV2/8 vector. The scFv was chosen over the IgG1 for incorporation into the vector due to the lack of Fc region and small size. Indeed, the limited capacity for this vector (1.5 kb) meant that it was not possible to insert the full antibody (2.5 kb), without compromising expression levels by removing the WPRE or substituting the promoter for a potentially weaker one. An amelioration of CNV was seen in mice injected with this vector. Importantly, we observed that, despite the fact that the bleb formed during subretinal injection only covered around one-third of the retinal area, even CNV lesions distal to the injection site were also suppressed. It appears that the AAV2/8 and/or antibodies are able to diffuse to the site of disease. This is important for translation to human patients. By using a secreted antibody it may not be necessary to transduce every target cell in the eye to generate a therapeutic effect. Thus, this approach is more feasible than an intracellular gene replacement (e.g., Stargardt disease), where the aim is to transduce all target cells.

A similar CNV suppression was demonstrated in AAV and recombinant antibody-treated mice. Using an estimated volume of a mouse eye to be approximately 19 mm^3, we attempted to quantify the amount of anti-VEGF scFv protein in AAV2/8-treated eyes. 1,000 μg/mL was detected in eyes injected with AAV2/8 anti-VEGF scFv, while we estimate that 80 μg anti-VEGF scFv protein injected during the antibody treatment experiments would correspond to

around 4,000 μg/mL antibody in the eye. Therefore, despite the fact that there was less scFv in the virus-treated mice, it seemed to be equally effective. This may be explained by this initial peak concentration quickly decreasing due to the decay of protein injected, while with AAV anti-VEGF scFv the levels will remain constant, as any degraded protein is continuously replenished. Another factor may be that the distance to CNV from the RPE-photoreceptor cells expressing the antibody is less than the vitreous location of antibody injections.

One cause for concern in our study was the detection of anti-VEGF scFv both in the serum- and in control AAV-injected eyes, as systemic inhibition of angiogenesis could lead to unwanted side effects. While the blood-retina barrier is normally responsible for keeping the eye an isolated organ, in CNV this becomes leaky, potentially explaining the presence of antibody in serum- and control AAV-treated eyes. However, these levels were very low compared to those in the AAV-anti-VEGF-treated eye. Furthermore, the subretinal injection in mice was given through the choroid, which would compromise the outer blood retina barrier and allow egress of AAV particles into the choroidal vasculature. This would not occur to the same extent in humans because the subretinal injection would be given transvitreally, which can be done without penetrating the choroidal vasculature.[12] A range of doses would inform us of the optimum dose, i.e., the minimum dose needed for efficacy without being able to detect antibody in the serum.

Interestingly, systemic suppression of VEGF has been found in clinical trials using intravitreal ranibizumab and bevacizumab,[25] and these drugs are still considered safe for clinical use. Indeed, bevacizumab is also safely given systemically to cancer patients, suggesting that systemic inhibition of angiogenesis may not be a major issue. Efforts to minimize any potential side effects should be made, however. While the half-life of these antibodies has to our knowledge not been studied, in general the IgG format of an antibody has a longer half-life than its scFv counterpart. This is due in part to the IgG being above the renal threshold (and thus remaining in the blood) and the scFv being below (thus leaving the blood). In addition, IgG antibodies are actively recycled into the blood via their Fc domains by the Fc receptor FcRn. However, scFvs do not possess an Fc domain, so they are not subject to this system and, hence, have lower retention in the blood than IgG. While a shorter half-life could potentially adversely affect the efficacy of scFvs, this may be more than made up for by increased safety due to lower systemic levels (as well as enhanced diffusion). This could be explored further in phase I/II clinical trials.

We used the laser-induced CNV mouse model, as it has similarities to human wet AMD, is highly reproducible, and is extremely well characterized in a number of anti-VEGF studies to date. One limitation of our study is that it focuses on prevention as opposed to treatment of established disease, which would be more clinically relevant to AMD. Future work could include treating established disease, but this is complicated by finding a treatment window, as in the laser model CNV is short-lived and self-limiting[26] and AAV2/8 takes at least 2 weeks[13] to express transgene. Thus, in trials, it may be necessary to give an initial injection of antibodies until therapeutic levels of protein are expressed via AAV2/8.

The AAV2 sFlt01 gene therapy in wet AMD phase I trial by Rakoczy et al.[4] has demonstrated that VEGF blockade delivered by gene therapy is safe. However, while these are promising results, this is only a small group of patients (8) and a short time point (1 year). Our data suggest that AAV2/8 may provide an alternate vector choice. Indeed, this vector may transduce more cells and express higher than the AAV2 serotype. Another advantage of elevated expression is that fewer viral particles are needed for efficacy; thus, there is a reduced chance of vector-mediated toxicity.

As our aim is to produce safer transgenes, it was important investigate AAV vector toxicity. The ERG showed no significant difference was observed in virus-injected responses compared to PBS controls. This suggests the virus has no effect on visual function, and it is in agreement with previous reports,[27] where the injection of 6.8×10^9 gcs (10-fold higher than our dose) of AAV8 GFP did not alter ERG readings.

One exciting possibility for our future studies will be investigating combination therapies. Alternatives to antibody therapies may include vasoinhibin,[28] interleukin-27 (IL-27),[29] complement inhibitors such as sCD59,[30] and complement factor H (CFH),[31] all of which have been efficacious in animal models of wet AMD. The use of these therapies in the protein format as described in these reports still requires regular administration, however. This problem can be overcome similarly by incorporating them (either alone or in combination) into a gene therapy vector for a continuous source of protein after a single administration. We therefore believe anti-angiogenic gene therapy is worth pursuing as a way to successfully treat this extremely prevalent and blinding condition.

MATERIALS AND METHODS

All materials were obtained from Sigma-Aldrich (Poole, UK) unless otherwise indicated.

Animals

All animal procedures were performed in accordance with the ARVO Statement for the Use of Animals in Ophthalmic and Vision Research and under the authority of a UK Home Office License (Home Office Project License 30/2843). Female C57BL/6 mice were bred in-house (at the University of Southampton). Mice of the same age (range 3–4 months old) were used for each experiment. All animal studies have been approved by the local Institutional Review Board.

Cells and Tissue Culture

HDMECs (Promocell, Heidelberg, Germany) were grown in complete MV Endothelial Cell Media (Promocell). HEK293T cells (ATCC) were grown in DMEM + 10% fetal calf serum (FCS) + 100 units/mL penicillin + 100 μg/mL streptomycin. Humidified incubators at 37°C and 5% CO_2 were used for culturing 293T cells and

HDMECs. 293F cells (Invitrogen, Inchinnan, UK) were grown in 293 Freestyle medium (Invitrogen) in Erlenmeyer flasks in shaking (130 rpm) humidified incubators at 37°C and 8% CO_2.

Antibody Cloning and Production

The G6-31 anti-VEGF (Liang et al.)[20] was used as a basis for both our antibodies. The variable heavy (V_H) domain of the anti-VEGF antibody was cloned into a plasmid (pEE14.1)[32] containing the mouse IgG1 heavy-chain constant domains. Into the same vector (at a separate location), the variable light (V_L) domain of the anti-VEGF antibody was cloned adjacent to the mouse IgG1 light-chain constant domains. Thus, when transfected into cells, this vector produces heavy and light chains separately, which then associate to form the mature antibody. The scFv format anti-VEGF was cloned by inserting the V_H and V_L domains of G6-31 separated by a 15-amino acid glycine-serine-rich flexible linker into the pcDNA4 HisMax plasmid (Invitrogen). This linker allows the association of the V_H and V_L domains to form a scFv capable of antigen binding. This plasmid contains a six-histidine-amino acid run at the N terminus of the scFv (His tag), used as a detection agent and for protein purification purposes. In addition, we cloned a CD33 (kindly provided by Claude Chan, University of Southampton) signal peptide upstream of the scFv to allow secretion of the protein.

The above plasmids were used to make recombinant IgG1 or scFv proteins, by spinning down 5×10^8 293F cells and resuspending in 25 mL medium containing 500 μg plasmid and 1.5 mg linear polyethylenimine (PEI; Park Scientific, Maidenhead, UK). This mix was returned to culture for 3 hr, before adding 475 mL medium and valproic acid to a final concentration of 3.75 mM. The transfection was cultured for 7 days, and supernatant was harvested by spinning the cells at 2,400 × *g* for 1 hr.

Antibody Purification

Anti-VEGF IgG1 was purified by affinity chromatography by virtue of the ability of the antibody to bind protein A. Running buffer (40 mM Tris-HCl, 2 mM EDTA, and 200 mM NaCl) was passed down a column (at 2 mL/min) containing protein A agarose beads (GE Healthcare, Little Chalfont, UK), before passing the 0.2-μm-filtered supernatant through. The column was washed with 30 mL running buffer, before eluting with 20 mL elution buffer (100 mM glycine, 1 mM EDTA, and 44 mM HCl [pH3]). To neutralize the pH of the eluate, 10 mL 5× running buffer was added after elution.

Anti-VEGF scFv was also purified by affinity chromatography. As His-tagged proteins bind Ni-conjugated beads, we exploited this for the purification of scFv protein. Supernatants were supplemented with 300 mM NaCl and 10 mM imidazole, and the pH was adjusted to pH 8 before 0.2-μm filtering to sterilize. To this, 3 mL Ni-NTA agarose (QIAGEN, Manchester, UK) and 1 mL Protease Inhibitor Cocktail Set III, EDTA-Free (Roche, Welwyn, UK) was added and left rotating overnight at 4°C. Then, the supernatant (plus Ni-agarose) was passed down an Econo-Column chromatography column (Bio-Rad, Hemel Hempstead, UK), where the agarose collected at the bottom while allowing fluid to pass through (under gravity). The Ni-agarose was then washed with 2 × 8 mL wash buffer (300 mM NaCl, 50 mM NaH_2PO_4, and 20 mM imidazole [pH 8]), and protein was eluted with 8 mL elution buffer (300 mM NaCl, 50 mM NaH_2PO_4, and 250 mM imidazole [pH 8]). Purified antibodies were dialyzed by inserting into Slide-A-Lyzer G2 3k MWCO dialysis cassettes (Invitrogen) and placing in an excess of PBS, with constant stirring overnight at 4°C. To concentrate antibodies, Amicon Ultra-15 3k MWCO Centrifugal Filter Units (Millipore, Livingstone, UK) were used according to the manufacturer's instructions.

Endotoxin Testing of Antibodies

An EndosafePTS machine with an Ameobocyte Lysate cartridge (both Charles River, Tranent, UK) was used according to the manufacturer's instructions to test the antibodies for endotoxin before use *in vivo*. Samples <10 EUs/mL/mg were deemed endotoxin free.

ELISA

Anti-VEGF-binding ability of antibodies was analyzed by ELISA. A 96-well ELISA plate (Fisher, Loughborough, UK) was coated by incubating at 4°C overnight with 1 μg/mL hVEGF or mVEGF (Abcam, Cambridge, UK) in PBS. The plate was then blocked by incubating at 37°C for 1.5 hr in 2% Marvel+PBS. Samples for anti-VEGF testing were prepared in blocking buffer and placed into wells in duplicate, incubating at 37°C for 1.5 hr. Anti-VEGF IgG1 was detected using rabbit anti-mouse conjugated to horseradish peroxidase (HRP) diluted 1:2,000 in blocking buffer, incubating at room temperature (RT) for 1 hr. Anti-VEGF scFv was detected with mouse anti-His tag HRP (Invitrogen) diluted 1:5,000 in blocking buffer, incubating at RT for 1 hr. After each step above, the plate was washed three times with PBS+0.05% Tween 20. The HRP substrate was made by dissolving an O-phenylenediamine dihydrochlorine (OPD) tablet in 100 mL of 4.8 g/L citric acid + 7.1 g/L Na_2HPO_4 + 0.012% H_2O_2. After adding HRP substrate and allowing color to form at RT in the dark, the reaction was stopped with 2.5 M H_2SO_4 and read on a plate reader (Dynatech MR4000, Dynatech Labs, Texas, USA) at 490 nm.

For antibody quantification in homogenized eyes by ELISA, an average diameter of adult C57BL/6 eyes of 3.3 mm[33] was used was used to calculate the volume (19 mm^3), equivalent to 19 μL.

SDS-PAGE

Samples were prepared by adding loading buffer (Bio-Rad) to samples (2:1) and heating at 95°C for 5 min. If denaturation was required, loading buffer + 5% β-mercaptoethanol was used. 10-μL samples including Novex Sharp Pre-stained Protein Standard were loaded onto Bis-Tris 10% ready-made gels (both Invitrogen). The gel was run in an XCell SureLock Mini-Cell (Invitrogen) at 200 V for 1 hr in MOPS buffer (50 mM 3-(N-morpholino)propanesulfonic acid, 50 mM Tris Base, 0.1% SDS, and 1 mM EDTA [pH 7.7]). Gels were stained with EZBlue according to the manufacturer's instructions to visualize bands. Images of gels were taken with a Hewlett Packard (Newcastle, UK) scanner.

Western Blotting

Samples were first run on an SDS-PAGE gel as above. Then, the gel was transferred onto nitrocellulose (0.45 μM; Bio-Rad) by removing from its case and placing in a sandwich of gel and nitrocellulose surrounded by filter papers in transfer buffer (Tris base [0.025 M], glycine [0.192 M], 1% SDS [pH 8.6], and 20% methanol). The sandwich was then run in an XCell II Blot Module (Invitrogen) at 100 V for 1 hr. After transfer, the nitrocellulose was blocked by placing in TBS (50 mM Tris and 150 mM NaCl [pH 7.6]) + 3% BSA at 4°C, overnight, with shaking.

Following blocking, the anti-His HRP detection antibody was added at RT for 2 hr, at a dilution of 1:5,000 in blocking buffer. This was then washed off with 3 × 5-min washes with TBS + 0.1% Tween20, before finally placing in TBS. Signals were then developed for imaging by adding enhanced chemiluminescence (ECL) reagent (Clarity Western ECL reagent, Bio-Rad). Images were captured using a Gel Doc (Bio-Rad).

Bioassay

0.5×10^4 HDMECs in complete medium were added to each well of a 96-well tissue culture plate (Fisher Scientific). The next day, medium was replaced with basal medium + 1% FCS. 1 day later, 10 ng/mL hVEGF in basal medium + 1% FCS were added, with or without antibodies. Antibody concentration ranged from 625 to 0.2 ng/mL, with 1:4 dilutions across the plate. The following antibodies were added in triplicate: anti-VEGF IgG1, anti-VEGF scFv, bevacizumab (positive control, Genentech, California, USA), and anti-PDGFRβ IgG1 (negative control). 2 days later, the number of live cells was quantified by adding the cell proliferation reagent WST-1 (Roche) for 4 hr and reading on a plate reader at 450 nm.

Laser-Induced CNV

Mice were anesthetized by intraperitoneal (i.p.) injection of 6 mg/mL ketamine plus 0.05 mg/mL Dexdormitor at a volume of 0.1 mL/10 g mouse. Pupils were dilated by the addition of G.tropicamide 1% eye drops followed by G.phenylephirine 2.5% eye drops. Eyes were coated with Viscotears to keep moist. A layer of Viscotears was used for coverslip adherence on the eye. Using a 532-nm retinal laser (frequency doubled ND-YAG laser, Zeiss, Welwyn, UK) set at 120 MW for 100 ms and spot size of 100 μm, four laser spots per eye (one per quadrant) were applied. Mice were recovered by injecting 0.3 mL of 0.5 mg/mL Antisedan (all materials in this section were obtained from Centaur Services, Castle Cary, UK).

Treatment with Anti-VEGF Antibody

Mice were anesthetized and pupils dilated using the same methods as above. With the aid of an operating microscope (Zeiss), 2 μL 20 mg/mL antibody (in PBS) was injected intravitreally with a 5-μL Hamilton syringe (Esslabs, Hadleigh, UK) fitted with a 34G needle (Esslabs). For each mouse, anti-VEGF scFv or anti-VEGF IgG1 (n = 6 or n = 5, respectively) was injected into one eye and an equal volume of PBS in the other (control) eye.

FFA

At 10–14 days after laser administration, mice were anesthetized and pupils dilated as above. The mouse was placed on the heated platform of a Micron III camera (Phoenix Labs, Pleasanton, USA). The retina was focused with the camera lens objective against the eye. 0.3 mL 2% fluorescein (Centaur Services) was injected i.p. The excitation and filter wheel was set to position 2. Early (30-s) and late (3-min) FFA images were captured for each eye using Streampix version (v.)5 software (Phoenix Labs).

Collagen IV IH

Mice were culled by cervical dislocation, and eyes for flat mounts were removed with forceps and fixed in 4% paraformaldehyde (PFA) for 30 min, before storing in PBS. Eyes were dissected so that only RPE-choroid remained. To enable the eyecup to be spread flat, four radial cuts in the sclera-choroid-RPE were made. Eyecups were washed four times in PBS, before blocking with 15% normal goat serum IH buffer (PBS + 0.2% Tween + 0.5% BSA), with shaking on an orbital shaker at 100 rpm overnight at 4°C. Samples were then incubated with a 1:500 dilution of rabbit anti-collagen IV (Abcam) in IH buffer for 2 days shaking at 4°C. Samples were washed four times in PBS, before incubating with a 1:200 dilution of goat anti-rabbit Alexafluor594 (Invitrogen) in IHC buffer for 1 day at 4°C. Samples were washed three times in PBS, mounted on a Superfrost Plus slide (Fisher Scientific) in 0.25 mL pre-warmed mowiol+citifluor (16% Mowiol; Harlow Chemicals, Batley, UK) in 30% glycerol in PBS plus 0.1% citifluor (VWR, Lutterworth, UK), and sealed with a coverslip. Slides were incubated overnight at 4°C in the dark to dry. Images were taken using a Zeiss Axioskop fluorescent microscope.

Quantification and Statistics

Quantification of size and intensity of lesions of both FFA and IH were done using ImageJ (version 1.47)[21] as described in Wigg et al.[34] Briefly, a region of interest (ROI) was drawn around the CNV lesion, and the signal intensity and area were measured. The area was multiplied by the signal intensity. A second ROI of the same area was drawn around an area without lesions and measured. This background measurement was subtracted from the lesion signal to give corrected values. The corrected signals for each eye were then summed and logged into a spreadsheet (GraphPad Prism). The "n" numbers thus refer to numbers of eyes used in each treatment group. An equal number of treated and control eyes was used. A box and whiskers graph was generated, with minimum and maximum values in each group illustrated by the whiskers and the band in the box representing the median. A Mann-Whitney test (two tailed) was used to determine a statistically significant difference in the two groups. Thus, a p value < 0.05 was classed as statistically significant.

AAV2/8 scFv Cloning

The anti-VEGF scFv or negative control scFv (Bcl-1) was cloned into the pAAV CAG WPRE vector (Vector Biolabs, Malvern, USA) between the CAG promoter and the WPRE region. The CD33 signal peptide was also included. XL10-Gold bacteria (Agilent, Cheadle,

UK) were used for AAV vector cloning to maintain the integrity of the inverted terminal repeats (ITRs) throughout the cloning process, which was confirmed by XmaI digestion (both ITRs contain XmaI sites).

AAV2/8 scFv Vector Production

For co-transfecting HEK293T cells with pAAV CAG scFv WPRE and pDP8.ape (Plasmid Factory, Bielefeld, Germany) in a 10-layer HyperFlask, a total of 500 μg DNA was added to 1.125 mg branched PEI. After growing for 72 hr in DMEM + 2% heat-inactivated serum, the transfected cells were harvested by centrifuging for 10 min at 1,200 × *g* at 20°C. The cell pellet was resuspended with 15 mL lysis buffer (1 M tris(hydroxymethyl)aminomethane and 150 mM NaCl), containing one protease inhibitor pellet (Roche). The cells were then lysed by three freeze-thaw cycles: samples were placed in a −80°C freezer for 1 hr, and then the sample was placed in a 37°C water bath for 15 min to thaw. Benzonase (Millipore) was added to the lysate to give a final concentration of 50 U/mL. This was incubated at 37°C for 45 min. The lysate was centrifuged at 3,700 × *g* for 20 min at RT. To isolate the AAV particles, an iodixanol gradient was used. The iodixanol gradients were made by layering the different percentages into a tube as follows: 7.2 mL of a 15% preparation was pipetted into the ultracentrifuge tube (OptiSeal 32.4-mL tubes; Beckman Coulter, Wycombe, UK). Then 4.8 mL of a 25% preparation was layered below the 15% fraction. The process was repeated to add 4 mL of a 40% preparation beneath the 25% fraction, and finally 4 mL of the 60% preparation was added beneath the 40% fraction. The lysate was added drop by drop to the top of the iodixanol gradient, and it was centrifuged at 357,653 × *g* for 1 hr and 30 min at 20°C. A 5-mL syringe attached to an 18G needle was used to pierce the ultracentrifuge tube with the needle at the interface between the 60% and 40% phases. As much of the 40% phase as possible was collected without collecting debris from the 25% phase.

To concentrate the isolated AAV vectors, 5 mL PBS was added to an Amicon Ultra 100K filter (Millipore) and centrifuged at 3,000 × *g* for 15 min at 20°C. 5 mL PBS was added to the collected iodixanol fraction (2–3 mL), and the total volume was added to the filter and centrifuged at 3,000 × *g* at 20°C until the volume reduced to 500 μL. 15 mL PBS was added to the filter and centrifuged at 3,000 × *g* at 20°C until the volume again reduced to 500 μL. This step was repeated twice more. On the third and final PBS wash, the volume was reduced to 250 μL. 50-μL aliquots of this purified AAV were stored at −80°C.

Confirmation of AAV2/8 scFv and Titering

To ensure that AAV was present in the purified sample, 10 μL purified virus was run on an SDS-PAGE gel, and bands were visualized as in SDS-PAGE above to show whether three bands corresponding to the three main AAV proteins (VP1-3) were present. The titer of the virus was determined by qPCR, with a forward primer complementary to the CAG promoter and a reverse primer complementary to the WPRE region. A standard curve was generated with varying concentrations of the plasmid DNA that was used to make the virus. The sample titer was determined by extrapolating the signal obtained from the standard curve and was expressed in genome copies.

In Vitro Testing of AAV2/8 scFv

To test the ability of the AAV2/8 scFv to successfully transduce cells, HEK293T cells were placed in a 6-well plate (Fisher Scientific) at a density of 5×10^5 cells per well. After 1 day the cells were rinsed in serum-free media before adding 1 mL serum-free media containing virus and 200 nM doxorubicin. This was incubated for 1 hr. Then 1 mL media with 20% FCS and doxorubicin was added and incubated at 37°C and 5% CO_2 for 2 days. Supernatant from these cells was analyzed for presence of antibody by ELISA and western blotting. An MOI of 100,000 was used.

In Vivo Testing of AAV2/8 scFv

AAV administration was performed as in Treatment with Anti-VEGF Antibody above, except that the injection was subretinal. A dose of 2 μL 4×10^8 gcs/μL (i.e., total 8×10^8 gcs) AAV2/8 anti-VEGF scFv was injected into one eye (n = 7), and an equal dose of AAV2/8 control scFv was injected into the other eye. To avoid virus particle adherence to the needles, surfactant was added (0.001% pluronic F68). At 3 and 8 weeks post-injection, laser was applied and FFA and IH were performed as above.

Homogenization of Eyes

Injected eyes were removed to 100 μL PBS + 1% Protease Inhibitor Cocktail Set III (Roche) and snap frozen whole in liquid N_2. Eyes were then thawed on ice and manually homogenized using a ground glass mortar and pestle tissue homogenizer (Mini Glass Homogenizer 3 mL with Handle, Camlab, Cambridge, UK). The homogenate was centrifuged at 16,000 × *g* for 35 min at 4°C to pellet the insoluble material, and the supernatant was stored at −80°C.

Obtaining Serum

Mice were placed under terminal anesthesia with CO_2, and then blood was removed by inserting a 25G needle attached to a 1-mL syringe into the heart (cardiac puncture). The blood was transferred to a 1.5-mL eppendorf tube, and allowed to clot at 4°C overnight. The samples were then spun at 2,000 × *g* for 20 min at 4°C, and the supernatant (serum) was removed and stored at −80°C.

Toxicity Experiments

To assess any toxicity of the subretinal injections, ERG measurements (visual function tests) were taken using the Micron ERG system (Phoenix Labs) 4 weeks after the administration of 2 μL 4×10^8/μL AAV2/8 anti-VEGF scFv (without PF68), i.e., the same dose as used for therapy experiments (n = 4). Additionally, ERG was performed on mice with 2 μL PBS + 0.001% pluronic F68 [n = 3]) and 2 μL PBS without surfactant (n = 3) injected subretinally.

ERG

All mice were dark adapted for 3 hr before ERG measurements (Figure 5) were obtained for study and control eyes. Scotopic b-wave amplitude, which reflects bipolar cell activity, was measured

from the trough of the a-wave to the peak of the b-wave. The photoreceptor-mediated a-wave was measured from the baseline to the trough of the a-wave. Differences between study and control eyes were compared with the nonparametric Mann-Whitney 2-tailed tests. ERG data are expressed as the mean ± 95% confidence interval (CI). A p value less than 0.05 was considered statistically significant.

IHC

The presence anti-VEGF scFv in AAV-injected eyes was also confirmed by IHC. Eyes from the toxicity experiment above were fixed as for IH. Eyes were then processed through a rising sucrose gradient, 30 min for each concentration, 5%, 10%, 12.5%, and 15%, before being left in 20% sucrose overnight. The anterior pole of the eye was dissected away, leaving the retina, choroid, and sclera intact. These posterior poles were embedded in optimal cutting temperature (OCT) matrix (Agar Scientific, Stansted, UK) and frozen. Sections were cut on a cryostat at −22°C, 16 μm thick, onto SuperfrostPlus slides (Fisher Scientific).

For staining sections, the tissue slices were surrounded using an ImmEdge Pen (Fisher Scientific) before drying for 20 min at 37°C. 200 μL blocking serum (5% goat serum in PBS with 0.3% Triton) was added, and slides were incubated for 30 min at RT. Blocking serum was then replaced with 200 μL anti-His G (Invitrogen; 1:100 in blocking serum) and incubated overnight at 4°C. After washing twice with PBS (5 min), 200 μL goat anti-mouse Alexafluor 555 (Fisher Scientific; 1:200 in PBS-Triton) was added and incubated in the dark at RT for 1 hr. The slides were washed twice with PBS and once with distilled water (5 min), before applying DAPI stain (5 μg/mL) for 6 min. Subsequently, slides were washed twice with distilled water, before drying and mounting coverslips with mowiol (Harlow Chemicals) and sealing with nail varnish.

Stained slides were imaged on a Leica DMi8 Confocal Microscope with an HC PL APO CS2 x20/0.75 IMM oil immersive objective with a 600-Hz scan speed, using Leica Application Suite X (2.0.1.14392). DAPI (blue) was detected using a UV 405-nm diode laser. The emission spectrum detected was 410–566 nm with a gain of 612.2 and an offset of −1.33. Alexafluor 555 (green) was detected using a DPSS 561 laser. The emission spectrum detected was 566–746 nm with a gain of 450.4 and an offset of −0.61. They were exposed sequentially between lines to prevent crosstalk between dyes.

SUPPLEMENTAL INFORMATION

Supplemental Information includes two tables and can be found with this article online at https://doi.org/10.1016/j.omtm.2018.11.005.

AUTHOR CONTRIBUTIONS

C.P.H. conduced the laboratory experiments with assistance from N.M.J.O., M.G., M.E.M., J.A.S., and S.G. and contributed to manuscript preparation. R.E.M. led the development and construction of viral vectors with assistance from M.E.M. and contributed to manuscript preparation. S.G., M.J.G., and A.J.L. contributed to study design, project oversight, analysis, and manuscript preparation. A.J.L. secured Gift of Sight funding for the project.

ACKNOWLEDGMENTS

This work was supported by the Gift of Sight charity. Gift of Sight is managed by the University of Southampton Exempt Charity (Inland Revenue reference number X19140). M.E.M. is funded by an MRC DPFS grant awarded to R.E.M. (MR/K007629/1) to develop AAV8 retinal gene therapy, and the vector facilities are funded by the Oxford University Hospitals NHS Foundation Trust NIHR Biomedical Research Centre. We would like to thank Claude Chan for providing help and advice with producing the antibodies and Savannah Lynn for working on the graphs (both University of Southampton).

REFERENCES

1. van Lookeren Campagne, M., LeCouter, J., Yaspan, B.L., and Ye, W. (2014). Mechanisms of age-related macular degeneration and therapeutic opportunities. J. Pathol. *232*, 151–164.
2. Hutton, D., Newman-Casey, P.A., Tavag, M., Zacks, D., and Stein, J. (2014). Switching to less expensive blindness drug could save medicare part B $18 billion over a ten-year period. Health Aff. (Millwood) *33*, 931–939.
3. Chakravarthy, U., Harding, S.P., Rogers, C.A., Downes, S., Lotery, A.J., Dakin, H.A., Culliford, L., Scott, L.J., Nash, R.L., Taylor, J., et al. (2015). A randomised controlled trial to assess the clinical effectiveness and cost-effectiveness of alternative treatments to Inhibit VEGF in Age-related choroidal Neovascularisation (IVAN). Health Technol. Assess. *19*, 1–298.
4. Rakoczy, E.P., Lai, C.M., Magno, A.L., Wikstrom, M.E., French, M.A., Pierce, C.M., Schwartz, S.D., Blumenkranz, M.S., Chalberg, T.W., Degli-Esposti, M.A., and Constable, I.J. (2015). Gene therapy with recombinant adeno-associated vectors for neovascular age-related macular degeneration: 1 year follow-up of a phase 1 randomised clinical trial. Lancet *386*, 2395–2403.
5. Campochiaro, P.A., Nguyen, Q.D., Shah, S.M., Klein, M.L., Holz, E., Frank, R.N., Saperstein, D.A., Gupta, A., Stout, J.T., Macko, J., et al. (2006). Adenoviral vector-delivered pigment epithelium-derived factor for neovascular age-related macular degeneration: results of a phase I clinical trial. Hum. Gene Ther. *17*, 167–176.
6. Cesana, D., Ranzani, M., Volpin, M., Bartholomae, C., Duros, C., Artus, A., Merella, S., Benedicenti, F., Sergi Sergi, L., Sanvito, F., et al. (2014). Uncovering and dissecting the genotoxicity of self-inactivating lentiviral vectors in vivo. Mol. Ther. *22*, 774–785.
7. Stieger, K., Le Meur, G., Lasne, F., Weber, M., Deschamps, J.Y., Nivard, D., Mendes-Madeira, A., Provost, N., Martin, L., Moullier, P., and Rolling, F. (2006). Long-term doxycycline-regulated transgene expression in the retina of nonhuman primates following subretinal injection of recombinant AAV vectors. Mol. Ther. *13*, 967–975.
8. Mao, Y., Kiss, S., Boyer, J.L., Hackett, N.R., Qiu, J., Carbone, A., Mezey, J.G., Kaminsky, S.M., D'Amico, D.J., and Crystal, R.G. (2011). Persistent suppression of ocular neovascularization with intravitreal administration of AAVrh.10 coding for bevacizumab. Hum. Gene Ther. *22*, 1525–1535.
9. Askou, A.L., Pournaras, J.A., Pihlmann, M., Svalgaard, J.D., Arsenijevic, Y., Kostic, C., Bek, T., Dagnaes-Hansen, F., Mikkelsen, J.G., Jensen, T.G., and Corydon, T.J. (2012). Reduction of choroidal neovascularization in mice by adeno-associated virus-delivered anti-vascular endothelial growth factor short hairpin RNA. J. Gene Med. *14*, 632–641.
10. Lai, C.M., Shen, W.Y., Brankov, M., Lai, Y.K., Barnett, N.L., Lee, S.Y., Yeo, I.Y., Mathur, R., Ho, J.E., Pineda, P., et al. (2005). Long-term evaluation of AAV-mediated sFlt-1 gene therapy for ocular neovascularization in mice and monkeys. Mol. Ther. *12*, 659–668.
11. Cashman, S.M., Ramo, K., and Kumar-Singh, R. (2011). A non membrane-targeted human soluble CD59 attenuates choroidal neovascularization in a model of age related macular degeneration. PLoS ONE *6*, e19078.
12. MacLaren, R.E., Groppe, M., Barnard, A.R., Cottriall, C.L., Tolmachova, T., Seymour, L., Clark, K.R., During, M.J., Cremers, F.P., Black, G.C., et al. (2014). Retinal gene

therapy in patients with choroideremia: initial findings from a phase 1/2 clinical trial. Lancet *383*, 1129–1137.

13. Lebherz, C., Maguire, A., Tang, W., Bennett, J., and Wilson, J.M. (2008). Novel AAV serotypes for improved ocular gene transfer. J. Gene Med. *10*, 375–382.
14. Murinello, S., Mullins, R.F., Lotery, A.J., Perry, V.H., and Teeling, J.L. (2014). Fcγ receptor upregulation is associated with immune complex inflammation in the mouse retina and early age-related macular degeneration. Invest. Ophthalmol. Vis. Sci. *55*, 247–258.
15. Tiller, K.E., and Tessier, P.M. (2015). Advances in Antibody Design. Annu. Rev. Biomed. Eng. *17*, 191–216.
16. Mordenti, J., Thomsen, K., Licko, V., Berleau, L., Kahn, J.W., Cuthbertson, R.A., Duenas, E.T., Ryan, A.M., Schofield, C., Berger, T.W., et al. (1999). Intraocular pharmacokinetics and safety of a humanized monoclonal antibody in rabbits after intravitreal administration of a solution or a PLGA microsphere formulation. Toxicol. Sci. *52*, 101–106.
17. Stahl, A., Stumpp, M.T., Schlegel, A., Ekawardhani, S., Lehrling, C., Martin, G., Gulotti-Georgieva, M., Villemagne, D., Forrer, P., Agostini, H.T., and Binz, H.K. (2013). Highly potent VEGF-A-antagonistic DARPins as anti-angiogenic agents for topical and intravitreal applications. Angiogenesis *16*, 101–111.
18. Souied, E.H., Devin, F., Mauget-Faysse, M., Kolar, P., Wolf-Schnurrbusch, U., Framme, C., Gaucher, D., Querques, G., Stumpp, M.T., and Wolf, S.; MP0112 Study Group (2014). Treatment of exudative age-related macular degeneration with a designed ankyrin repeat protein that binds vascular endothelial growth factor: a phase I/II study. Am. J. Ophthalmol. *158*, 724–732.e2.
19. Kovaleva, M., Ferguson, L., Steven, J., Porter, A., and Barelle, C. (2014). Shark variable new antigen receptor biologics - a novel technology platform for therapeutic drug development. Expert Opin. Biol. Ther. *14*, 1527–1539.
20. Liang, W.C., Wu, X., Peale, F.V., Lee, C.V., Meng, Y.G., Gutierrez, J., Fu, L., Malik, A.K., Gerber, H.P., Ferrara, N., and Fuh, G. (2006). Cross-species vascular endothelial growth factor (VEGF)-blocking antibodies completely inhibit the growth of human tumor xenografts and measure the contribution of stromal VEGF. J. Biol. Chem. *281*, 951–961.
21. Schneider, C.A., Rasband, W.S., and Eliceiri, K.W. (2012). NIH Image to ImageJ: 25 years of image analysis. Nat. Methods *9*, 671–675.
22. Miyazaki, J., Takaki, S., Araki, K., Tashiro, F., Tominaga, A., Takatsu, K., and Yamamura, K. (1989). Expression vector system based on the chicken beta-actin promoter directs efficient production of interleukin-5. Gene *79*, 269–277.
23. Donello, J.E., Beeche, A.A., Smith, G.J., 3rd, Lucero, G.R., and Hope, T.J. (1996). The hepatitis B virus posttranscriptional regulatory element is composed of two subelements. J. Virol. *70*, 4345–4351.
24. Campa, C., Kasman, I., Ye, W., Lee, W.P., Fuh, G., and Ferrara, N. (2008). Effects of an anti-VEGF-A monoclonal antibody on laser-induced choroidal neovascularization in mice: optimizing methods to quantify vascular changes. Invest. Ophthalmol. Vis. Sci. *49*, 1178–1183.
25. Chakravarthy, U., Harding, S.P., Rogers, C.A., Downes, S.M., Lotery, A.J., Culliford, L.A., and Reeves, B.C.; IVAN study investigators (2013). Alternative treatments to inhibit VEGF in age-related choroidal neovascularisation: 2-year findings of the IVAN randomised controlled trial. Lancet *382*, 1258–1267.
26. Tobe, T., Ortega, S., Luna, J.D., Ozaki, H., Okamoto, N., Derevjanik, N.L., Vinores, S.A., Basilico, C., and Campochiaro, P.A. (1998). Targeted disruption of the FGF2 gene does not prevent choroidal neovascularization in a murine model. Am. J. Pathol. *153*, 1641–1646.
27. Allocca, M., Mussolino, C., Garcia-Hoyos, M., Sanges, D., Iodice, C., Petrillo, M., Vandenberghe, L.H., Wilson, J.M., Marigo, V., Surace, E.M., and Auricchio, A. (2007). Novel adeno-associated virus serotypes efficiently transduce murine photoreceptors. J. Virol. *81*, 11372–11380.
28. Wakusawa, R., Abe, T., Sato, H., Sonoda, H., Sato, M., Mitsuda, Y., Takakura, T., Fukushima, T., Onami, H., Nagai, N., et al. (2011). Suppression of choroidal neovascularization by vasohibin-1, a vascular endothelium-derived angiogenic inhibitor. Invest. Ophthalmol. Vis. Sci. *52*, 3272–3280.
29. Hasegawa, E., Oshima, Y., Takeda, A., Saeki, K., Yoshida, H., Sonoda, K.H., and Ishibashi, T. (2012). IL-27 inhibits pathophysiological intraocular neovascularization due to laser burn. J. Leukoc. Biol. *91*, 267–273.
30. Bora, N.S., Kaliappan, S., Jha, P., Xu, Q., Sivasankar, B., Harris, C.L., Morgan, B.P., and Bora, P.S. (2007). CD59, a complement regulatory protein, controls choroidal neovascularization in a mouse model of wet-type age-related macular degeneration. J. Immunol. *178*, 1783–1790.
31. Kim, S.J., Kim, J., Lee, J., Cho, S.Y., Kang, H.J., Kim, K.Y., and Jin, D.K. (2013). Intravitreal human complement factor H in a rat model of laser-induced choroidal neovascularisation. Br. J. Ophthalmol. *97*, 367–370.
32. Harfst, E., Johnstone, A.P., Gout, I., Taylor, A.H., Waterfield, M.D., and Nussey, S.S. (1992). The use of the amplifiable high-expression vector pEE14 to study the interactions of autoantibodies with recombinant human thyrotrophin receptor. Mol. Cell. Endocrinol. *83*, 117–123.
33. Remtulla, S., and Hallett, P.E. (1985). A schematic eye for the mouse, and comparisons with the rat. Vision Res. *25*, 21–31.
34. Wigg, J.P., Zhang, H., and Yang, D. (2015). A Quantitative and Standardized Method for the Evaluation of Choroidal Neovascularization Using MICRON III Fluorescein Angiograms in Rats. PLoS ONE *10*, e0128418.
35. Hansel, T.T., Kropshofer, H., Singer, T., Mitchell, J.A., and George, A.J. (2010). The safety and side effects of monoclonal antibodies. Nat. Rev. Drug Discov *9*, 325–338.